




## Short Report

# Spatiotemporally controlled induction of gene expression *in vivo* allows tracking the fate of tumor cells that traffic through the lymphatics

Nicole Grau<sup>1,2</sup>, Sandra D. Scherer<sup>1,2</sup>, Melanie Rothley<sup>1,2</sup>, Sven Roßwag<sup>2</sup>, Wilko Thiele<sup>1,2</sup>, Nikolas H. Stoecklein<sup>3</sup>, Natascha Cremers<sup>1,2</sup>, Sonja Thaler<sup>2</sup>, Boyan K. Garvalov<sup>2</sup> and Jonathan P. Sleeman <sup>1,2</sup>

<sup>1</sup>Institute of Toxicology and Genetics, Karlsruhe Institute of Technology (KIT), Campus Nord, Karlsruhe, Germany

<sup>2</sup>European Center for Angioscience (ECAS), Medical Faculty Mannheim, University of Heidelberg, Mannheim, Germany

<sup>3</sup>Department of General, Visceral and Pediatric Surgery, Medical Faculty, University Hospital of the Heinrich-Heine-University Düsseldorf, Düsseldorf, Germany

Metastasis is a multistep process, during which circulating tumor cells traffic through diverse anatomical locations. Stable inducible marking of tumor cells in a manner that is tightly spatially and temporally controlled would allow tracking the contribution of cells passing through specific locations to metastatic dissemination. For example, tumor cells enter the lymphatic system and can form metastases in regional lymph nodes, but the relative contribution of tumor cells that traffic through the lymphatic system to the formation of distant metastases remains controversial. Here, we developed a novel genetic switch based on mild transient warming (TW) that allows cells to be marked in a defined spatiotemporal manner *in vivo*. Prior to warming, cells express only EGFP. Upon TW, the EGFP gene is excised and expression of mCherry is permanently turned on. We employed this system in an experimental pancreatic cancer model and used localized TW to induce the genetic switch in tumor cells trafficking through tumor-draining lymph nodes. Thereby we found that tumor cells disseminating *via* the lymphatics make a major contribution to the seeding of lung metastases. The inducible genetic marking system we have developed is a powerful tool for the tracking of metastasizing cells *in vivo*.

### Introduction

Cancer cells disseminating from primary tumors pass through different conduits and anatomical sites, which can affect the outcome of the metastatic process.<sup>1</sup> Dissecting the contribution of cells that traffic through distinct locations at specific points in time requires their labeling in a precise spatiotemporal manner, ideally using an inducible genetic switch that can permanently mark the disseminating cells. Current inducible

gene expression systems typically employ soluble inducers, such as tetracycline/doxycycline or (4-hydroxy)tamoxifen.<sup>2</sup> While such treatments allow temporal control of gene expression, spatial restriction of the induction is difficult to achieve, due to diffusion and systemic distribution of the inducer. Leakiness due to basal promoter activity is also often a problem. High spatiotemporal precision of cell labeling can be achieved using phototransformation of fluorescent proteins

**Additional Supporting Information** may be found in the online version of this article.

**Key words:** heat-inducible expression, genetic switch, metastasis, lymph node, cell tracking

**Abbreviations:** EGFP: enhanced green fluorescent protein; HSE: heat shock element; HSF: heat shock factor; HSP70: heat shock protein 70 kDa; HSPmin: minimal HSP70 promoter; IRES: internal ribosomal entry site; LN: lymph node; TNF $\alpha$ : tumor necrosis factor  $\alpha$ ; TW: transient warming; TWIGS: transient warming-induced genetic switch; VEGF-C: vascular endothelial growth factor C

**Conflict of interest:** The authors declare that they have no conflicts of interest.

**Grant sponsor:** Deutsche Forschungsgemeinschaft; **Grant number:** SPP1190

This is an open access article under the terms of the Creative Commons Attribution License, which permits use, distribution and reproduction in any medium, provided the original work is properly cited.

DOI: 10.1002/ijc.32766

**History:** Received 13 May 2019; Accepted 18 Oct 2019; Online 1 Nov 2019

**Correspondence to:** Jonathan P. Sleeman, E-mail: [sleeman@medma.uni-heidelberg.de](mailto:sleeman@medma.uni-heidelberg.de)

**What's new?**

Tracking tumor cells as they move through tissues on their way to colonizing distant organs can provide important insight into the metastatic process. Methods to accurately track tumor cell movement, particularly through the lymphatic system, however, have been lacking. Here, the authors developed a novel system employing a genetic switch from green fluorescent protein expression to red fluorescent protein expression to track tumor cells in an *in vivo* model. The switch, induced in a spatiotemporally controlled manner by mild transient warming, permanently marked tumor cells, allowing the cells to be successfully followed through the lymphatics to their final destinations.

after exposure to light of specific wavelength.<sup>3,4</sup> However, turnover of the phototransformed proteins means that cells labeled with them cannot be followed for more than a few days, which is insufficient for comprehensive characterization of tumor progression and metastasis.

Physical stimuli such as temperature modulation represent an alternative approach. Increased temperature activates transcription factors of the heat shock factor (HSF) family, which transactivate heat shock elements (HSEs) in the promoters of heat-sensitive genes, including heat-shock protein genes.<sup>5</sup> Such promoters are activated rapidly and efficiently in response to heat.<sup>6,7</sup> Importantly, in addition to precise temporal control, heat-responsive promoters can also be regulated in a spatially defined manner. This can be achieved by targeted application of electromagnetic radiation or focused ultrasound to deeper tissues, or *via* direct contact with a heat source for more superficially located targets.<sup>8</sup>

One important question that can be addressed through precise spatiotemporally controlled tumor cell labeling is the contribution of cells that traffic through lymph nodes to the formation of metastases. Tumor cells that disseminate *via* the lymphatics first pass through the lymph nodes (LNs) that drain the primary tumor. These cells may establish metastases in the LNs, or pass through them and continue to disseminate hematologically either by invading LN blood vessels<sup>4,9</sup> or by trafficking through the efferent lymphatics that empty into the blood circulation, for example *via* the thoracic duct. Similarly, established LN metastases may conceivably shed tumor cells into the blood system, either through the efferent lymphatics or through blood vessels within the LN. However, the degree to which tumor cells that disseminate *via* the lymphatic system contribute to metastasis formation in distant organs is insufficiently understood. LN metastases have been seen as potential reservoirs of tumor cells that could seed further metastases, and LNs regional to primary tumors have been surgically removed for decades with the aim of improving patient survival.<sup>10</sup> Furthermore, the expression of factors in primary tumors that stimulate lymphangiogenesis, such as VEGF-C, often correlates with LN metastasis formation and poor prognosis.<sup>10</sup> However, the contribution of tumor cells that traffic *via* the lymphatics to metastasis formation in vital organs remains controversial. A long-standing notion is that LNs may act as filters that impede the further passage of tumor cells.<sup>11</sup> Moreover, many long-term randomized trials

have failed to demonstrate that dissection or irradiation of LNs beyond the sentinel LNs has significant benefit for overall patient survival.<sup>12–17</sup>

Together, these observations underline the need for methods that accurately track the fate of tumor cells that traffic through the lymphatics, and permit their contribution to metastasis formation in vital organs to be evaluated. To address this issue, we report here a genetic tracking method that allows the fate of tumor cells trafficking through LNs *in vivo* to be assessed. In this method, tumor cells disseminating *via* the lymphatics are permanently marked *in vivo* through a switch in expression of green fluorescent protein to a red fluorescent protein, allowing their fate and behavior to be tracked. In a proof of principle experiment using a pancreatic cancer model, we found that a large proportion of lung metastases were seeded by tumor cells that had trafficked *via* the lymphatics.

**Materials and Methods****Cell culture, transfection and stable tumor cell lines**

The rat pancreatic carcinoma cell line BSp73-ASML, as well as the rat mammary carcinoma cell lines MT-450 and MTLy were maintained as described previously.<sup>18</sup> ASML-TWIGS cells were obtained by cotransfection of the HSP-Cre-IRES-Luc construct with a puromycin resistance plasmid using Lipofectamine 2000 (Thermo Fisher Scientific, Waltham, MA). Resistant clones were selected for luciferase induction 3 hr after TW, then cotransfected with the floxed EGFP-mCherry reporter construct and a neomycin resistance plasmid. Resistant clones with EGFP expression were picked and tested for switching to mCherry expression after TW. B16-F10 (RRID:CVCL\_0159) and MCF-7 (RRID:CVCL\_0031) cells were purchased from ATCC and cultured in DMEM with 10% FBS, 1% penicillin/streptomycin at 37°C with 5% CO<sub>2</sub>. B16-F10 cells were transfected with 5 µg HSPmin-Luc plasmid and 20 µl Lipofectamine 2000 and MCF-7 cells were transfected with 3 µg HSPmin-Luc plasmid and 10 µl FuGENE HD (Promega) in 6 cm plates, according to the manufacturer's instructions. MCF-7 cells were authenticated within the last 3 years by CLS Cell Lines Service (Eppelheim, Germany) using STR profiling. Experiments were performed with mycoplasma-free cells.

**Cloning**

*Cloning of the HSPmin element.* A 172 bp long fragment of the rat heat shock 70 kDa protein 1B (Hspa1b) promoter was

amplified by PCR with HSP-forward 5'-CAAGGGCGGTACCC TCAACATGG-3' and HSP-reverse 5'-GGAATCTGGTGTCC TGCGCGCCG-3' primers from rat genomic DNA, cloned into pCR2.1 (Topo-Cloning Kit, Invitrogen), then subcloned into the SacI/NotI sites of pBluescript to create the HSP-pBluescript construct.

**Cloning of HSPmin-Luc.** The HSPmin element was cut out of pCR2.1-Topo by HindIII and XhoI and ligated into the HindIII/XhoI sites of the promoterless luciferase reporter pXP2.

**Cloning of HSP-Cre-IRES-Luc.** The Cre open reading frame (ORF) of pPGK-Cre-bpA (kind gift from Kurt Fellenberg) was excised using XhoI and ligated into the XhoI site of HSP-pBluescript behind the HSPmin element creating the HSP-Cre construct. The HSPmin element-Cre portion of pBluescript-HSP-Cre was isolated after SacI digestion and blunt-ended. The mammalian expression vector MMTV-IRES-Luc (kind gift from Gerhard Christofori) was digested with SacI and PstI to remove the MMTV promoter. The residual vector was blunt-ended and ligated with the blunt-ended HSPmin element-Cre fragment.

**Cloning of floxed-EGFP/mCherry.** The mammalian expression vector pCall2-updated (kind gift from Gerhard Christofori) uses the ubiquitous CMV-IE-chicken  $\beta$  actin promoter to drive expression of a floxed  $\beta$ -Geo gene followed by EGFP. This vector was cut with XhoI and NotI to excise the EGFP cassette, then the residual vector was blunt-ended and recircularized (pCall2-updated  $\Delta$ EGFP construct). Next, the EGFP cassette in pEGFP-N1 (Clontech) was amplified by PCR using ClaI-EGFP 5'-GGCATCGATCCACAACCATGGT GAGCAAGGGCGAGGAGCTG-3' and EGFP-SphI 5'-GGCG CATGCTTACTTGACAGCTCGTCCATGCCGAGAGTGAT CCC-3' primers. The following cycling conditions were used: 3 min 94°C, 1 min 94°C; 1.5 min 72°C 30 $\times$ ; 10 min 72°C. The 750 bp PCR product was digested with ClaI and SphI, and ligated into pCall2-updated  $\Delta$ EGFP digested with ClaI and SphI, thereby replacing the  $\beta$ -geo gene with the EGFP cassette followed by a stop codon at the end of the coding sequence and three tandem polyadenylation signals to create the pCall2-updated  $\Delta$ EGFP  $\Delta\beta$ -geo EGFP construct. Finally, the open reading frame of the mCherry fluorescent protein was amplified from pcDNA3.1 mCherry (kind gift from Marcus Diefenbacher) by PCR using BglIII-mCherry 5'-GACAGATC TGCCACCATGGT GAGCAAGGGCGAGGAGCTG-3' and Cherry-stop-XhoI 5'-GACCTCGAGTCAACCCTCGTACA GCTCGTCCATGCCGAGAGTGATC-3' primers. The following cycling conditions were used: 3 min 94°C; 1 min 94°C; 1.5 min 72°C 30 $\times$ ; 10 min 72°C. The 800 bp PCR-product was digested with BglIII and XhoI and ligated into the BglIII/XhoI sites of the pCall2-updated  $\Delta$ EGFP  $\Delta\beta$ -geo EGFP construct to create the floxed EGFP-mCherry reporter construct.

All constructs were verified by sequencing.

### Transient warming *in vitro* and luciferase assays

TW of cell suspensions (100  $\mu$ l) for luciferase assays were performed in a PCR machine for 10 min at the indicated test temperature. Cells were then processed for luciferase assays.

For luciferase assays using cell lysates, lysates were prepared on ice for 10 min with a lysis buffer containing 0.1 M Tris pH 7.5, 2 mM EDTA, 1% Triton X-100. Lysate aliquots of 20  $\mu$ l were transferred in a 96-well assay plate and analyzed in a luminescence reader (VicorLight, Perkin Elmer). Before each measurement, an automated dispenser added 70  $\mu$ l assay buffer per well (1 mM DTT, 1 mM ATP, 25 mM glycylglycine, 15 mM MgSO<sub>4</sub>, 4 mM EGTA), followed by 20  $\mu$ l substrate buffer (200  $\mu$ M luciferin, 25 mM glycylglycine, 15 mM MgSO<sub>4</sub>, 4 mM EGTA). Alternatively, luciferase assays were performed using the above lysis buffer and reagents from the Luciferase Assay System (Promega, E1500) with a Spark microplate reader (Tecan). The luciferase signal (count/s) was normalized per  $\mu$ g of total protein in the lysates, as determined using the Pierce BCA Protein Assay (Thermo Fisher Scientific).

For luciferase assays with living cells to determine luciferase expression kinetics after TW, cells were seeded in triplicate in 96-well ViewPlates (Greiner Bio-One, Kremstünster, Austria) and luciferin-K<sup>+</sup> salt (Biosynth, Itasca, IL) was added to a final concentration of 0.5 mM. The plates were sealed with a translucent foil and placed in a luminometer (EnVision, Perkin Elmer, Waltham, MA) at 37°C. Measurements were taken every 15 min (as indicated) for 24 hr. Measurements were expressed in counts per second.

### Tumor experiments and TW *in vivo*

All studies were approved by the local Ethical Review Board. Unless otherwise indicated, groups of eight male 8–9 weeks old RNU/RNU rats (Charles River, Wilmington, MA) were injected subcutaneously in the flank with  $1 \times 10^6$  ASML-TWIGS cells in PBS per rat. Animals were then either left untreated or received one daily TW of the axillary LN ipsilateral or contralateral to the primary tumor from Day 1 after tumor cell injection until day 32 (see Supporting Information for details). Tumor size was measured with a caliper. Tumor volume was calculated using the formula  $\pi/6 \times L \times W \times H$ , where  $L$ ,  $W$  and  $H$  are length, width and height, respectively. The rats were sacrificed 32 days after injection of tumor cells or when tumor volumes reached the maximum permitted size. Primary tumors, axillary LNs and lungs were fixed in formalin and paraffin-embedded for histological analyses.

### Quantification of lung metastases

Macrometastases >0.1 mm in diameter on the surface of unfixed lung lobes were evaluated using an epifluorescence stereomicroscope (Leica). Metastases in which only EGFP-expressing cells were present were scored as EGFP<sup>+</sup>; metastases in which only mCherry-expressing cells or a mixture of EGFP<sup>-</sup> and mCherry-expressing cells were present were scored as mCherry<sup>+</sup>.

### Immunofluorescence

Paraffin sections were deparaffinized and enzymatic antigen retrieval was performed by incubation with 1.25 µg/ml Proteinase K (Roth, Karlsruhe) in TE buffer. EGFP-staining was done overnight at 4°C with 1.25 µg/ml anti-EGFP-antibody (polyclonal, #632376 Clontech) followed by incubation with an Alexa-488 labeled secondary antibody (4 µg/ml goat-anti-rabbit-F(ab')<sub>2</sub>, Dako, Glostrup Denmark) for 1 hr. Prior to mCherry staining, endogenous biotin was blocked using the Biotin Blocking System Kit (Dako, Glostrup Denmark). After blocking, the slides were incubated with 10 µg/ml biotin-labeled anti-RFP-antibody (polyclonal, Abcam ab34771) at 4°C overnight, then stained with 5 µg/ml Alexa-546 labeled streptavidin (Invitrogen, Karlsruhe) in TBS for 2 hr at room temperature. Nuclear staining was performed by incubation with 2 µg/ml Hoechst-33342 (Invitrogen, Karlsruhe) in water for 7 min. Cover slips were mounted with Mowiol 4–88 (Roth, Karlsruhe).

### Statistics

Error bars indicate standard error of the mean. When two groups were compared, a two-sided Student's *t*-test was used. For multiple comparisons, one-way ANOVA was used with Bonferroni *post hoc* tests for pairwise comparisons (GraphPad Prism). For comparing the proportions of metastases generated by EGFP<sup>+</sup> and mCherry<sup>+</sup> cells, pairs of treatments were compared using the Chi-square test (GraphPad Prism). Statistical significance is indicated by asterisks: \**p* < 0.05; \*\**p* < 0.01; \*\*\**p* < 0.001.

### Data availability

The data that support the findings of our study are available from the corresponding author upon reasonable request.

## Results

### Development of a green–red fluorescent protein genetic switch triggered by TW

To develop an inducible system for marking disseminating tumor cells in a spatiotemporally controlled manner, we first created a promoter element that can be activated by TW. Heat-regulated promoters are generally also activated by other stress factors found within tumors such as hypoxia.<sup>19</sup> To create a promoter that is induced specifically in response to TW but not hypoxia, we used a sequence of the rat HSP70 promoter containing a single heat shock response element (HSE I), which has been reported to show very little induction after hypoxia.<sup>20</sup> This minimal HSP70 promoter (HSPmin) was cloned in front of a luciferase reporter (HSPmin-Luc) to allow its activity to be characterized (Fig. 1a, top).

The HSPmin promoter was then used to create a Transient Warmth Inducible Genetic Switch (TWIGS) system, consisting of two plasmids (Fig. 1a, bottom). In the first construct (HSP-Cre-IRES-Luc), the HSPmin promoter drives expression of Cre recombinase, as well as luciferase *via* an internal

ribosome entry site (IRES). The second construct (floxed EGFP/mCherry) uses a strong constitutive CMV/β-actin promoter to drive expression of a floxed EGFP, which is followed by mCherry. At 37°C, cells transfected with the two TWIGS constructs only express EGFP. TW induces Cre expression, leading to excision of the floxed EGFP cassette and the switching on of mCherry expression.

MT450, ASML and MTLy tumor cell lines were stably transfected with HSPmin-Luc. ASML cells were also stably transfected with the TWIGS constructs. The cells were then subjected to various temperatures between 37°C and 44°C for 10 min. Luciferase reporter assays showed that the optimal activation temperature for the HSPmin element is around 43–43.5°C (Fig. 1b). After TW (hereafter defined as 10 min warming to 43.5°C), transactivation by the HSPmin element in living cells peaked at around 2 hr and returned to basal levels by 12 hr post-TW (Fig. 1c). Cells maintained at 37°C exhibited no luciferase activity over background (Fig. 1c), while TW induced the activity of the HSPmin-Luc reporter by up to 12-fold (Fig. 1d). Importantly, exposure of the HSPmin-Luc reporter cell lines to hypoxic conditions for 24 hr elicited no increase in luciferase reporter activity (Fig. 1d), although the same conditions led to a massive increase in the activity of a reporter driven by hypoxia response elements (Supporting Information Fig. S1), demonstrating that the HSPmin promoter element is not activated by hypoxia. It was also not induced by other common signals in the tumor microenvironment, including the major inflammatory mediator TNFα and the key lymphangiogenic factor VEGF-C (Supporting Information Fig. S2). Furthermore, TW did not affect the expression of the epithelial marker E-cadherin or the mesenchymal marker vimentin, indicating that it does not change general cellular properties involved in metastasis, such as EMT (Supporting Information Fig. S3). At the same time, the rat HSPmin promoter was activated by TW not only in rat ASML pancreatic carcinoma cells but also in the murine melanoma cells B16-F10 and the human breast carcinoma cells MCF-7 (Supporting Information Fig. S4), indicating that this system is applicable across different species and tumor entities.

Next, the ASML-TWIGS cell line was exposed to TW or hypoxia. In the absence of TW under normoxic conditions, only EGFP was expressed in these cells. TW induced a switch from EGFP to mCherry expression in the majority of the cells, but, importantly, no switch was induced by hypoxia (Fig. 1e), indicating that the HSPmin promoter element in the TWIGS system is tightly controlled in the absence of TW.

### TW activates the HSPmin element *in vivo*

To apply local TW to the axillary LNs of rats, a low-efficiency electric light bulb with an appropriate size and form to fit into the axilla of the rats was employed. When operated at a constant voltage, the surface temperature of the bulb was stable after 10 min (Fig. 2a) and proportional to the voltage applied (Fig. 2b). These data allowed us to establish that the optimal



temperature for inducing the HSPmin element (43–43.5°C) was achieved by applying a voltage of 63 V. To determine whether applying the light bulb to the axillary region is sufficient to activate the HSPmin element *in vivo*, ASML cells expressing luciferase under the control of the HSPmin element were injected subcutaneously into the flank of experimental

rats. Once the primary tumor grew and a palpable metastasis in the axillary LN ipsilateral to the primary tumor was detected, rats were anesthetized and an electric light bulb at 43.5°C was used to apply TW for 10 min to the ipsilateral axilla (Fig. 2c). No luciferase activity was detected by bioluminescence imaging before TW, but 3.5 hr afterward, there was strong luciferase

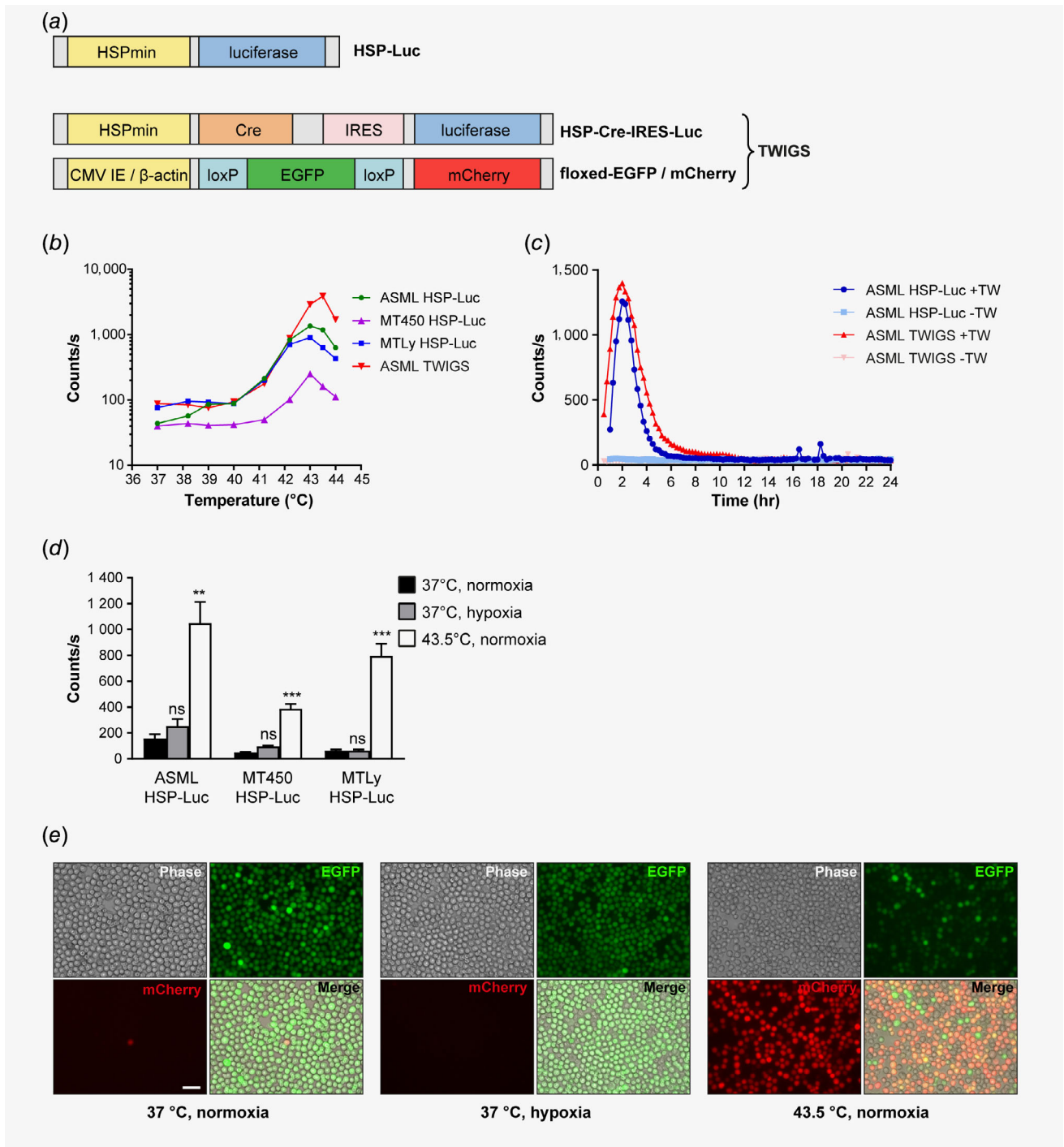
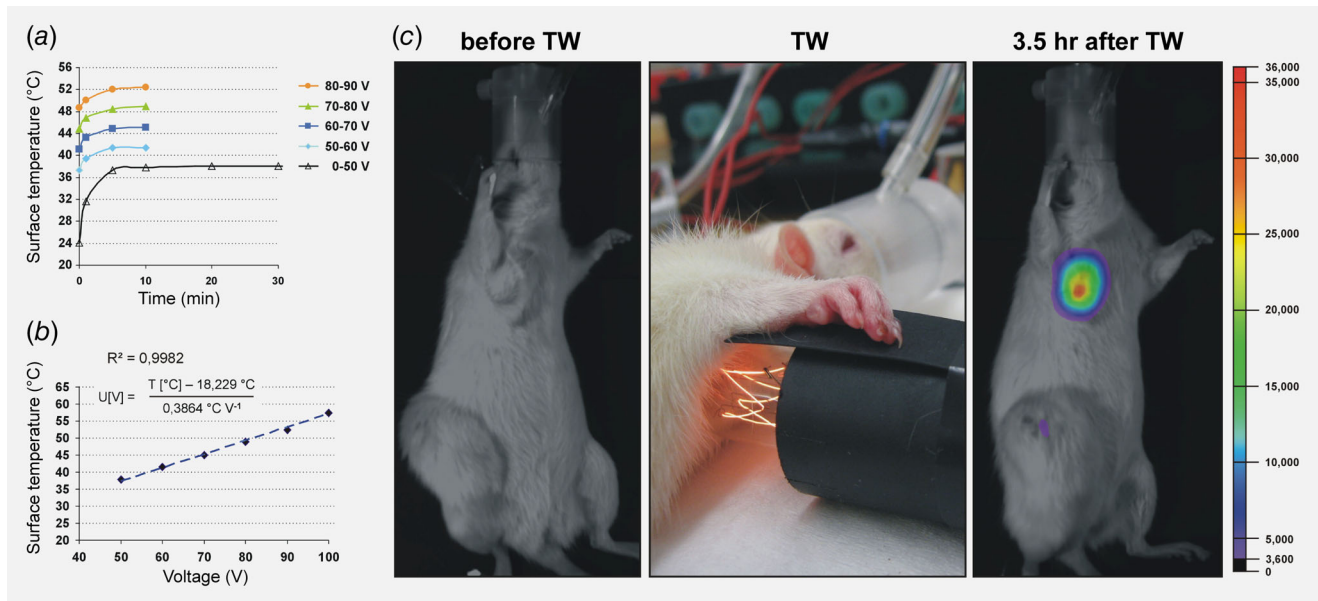


Figure 1. Legend on next page.



**Figure 2.** Induction of gene expression by TW *in vivo*. (a) The voltage of a Barthelme R1654 light bulb was first raised from 0 to 50 V and subsequently increased in 10 V steps as indicated. The surface temperature of the bulb was measured at different time points after raising the temperature to determine the kinetics of warming. A stable temperature was reached at all voltages after 10 min. (b) The surface temperature of the light bulb was measured 10 min after application of the indicated constant voltages. The measurement showed a very good fit ( $R^2 = 0,9982$ ) with a linear function, described by the equation shown. (c) ASML cells expressing luciferase under the control of the HSPmin element were transplanted subcutaneously in BDX rats. After the primary tumor had grown and palpable metastases in the ipsilateral lymph node were detected, the animals were imaged by bioluminescence (left). Subsequently, the axilla was exposed to TW by applying an electric bulb at 63 V (43.5°C) for 10 min (middle); 3.5 hr later, the animals were injected with luciferin (i.p.) and bioluminescence imaging was performed (right). [Color figure can be viewed at [wileyonlinelibrary.com](http://wileyonlinelibrary.com)]

induction at the site of warming (Fig. 2c). The primary tumor did not show luciferase activity, indicating that the induction is tightly regulated, both temporally and spatially, and only occurs after local TW *in vivo*.

### TW-induced EGFP-mCherry switch *in vivo* demonstrates a major contribution of tumor cells trafficking *via* the lymphatics to lung metastasis

In a proof of principle experiment, we used ASML cells stably transfected with the TWIGS constructs to determine the degree to which cells that traffic *via* the lymphatics contribute to lung metastasis formation. After the injection of the

ASML-TWIGS cells subcutaneously into the flank of experimental rats, the ipsilateral or contralateral axillary LNs were subjected to daily TW until the end of the experiment. Lungs were then examined for the presence of EGFP<sup>+</sup> and mCherry<sup>+</sup> metastases on their surface. Metastases derived from tumor cells that trafficked *via* the lymph nodes would be expected to express mCherry, whereas those that disseminated to the lung directly *via* the bloodstream should only express EGFP.

TW had no effect on the growth of the primary tumors (Fig. 3a), nor on the percentage of mCherry<sup>+</sup> cells in the primary tumor (Figs. 2b and 2e). The volume of the tumor-draining ipsilateral axillary LNs compared to the contralateral

**Figure 1.** Induction of a genetic switch under the control of a minimal HSP70 promoter by mild transient warming (TW). (a) Schematic representation of the HSPmin promoter-driven constructs used. HSPmin, minimal promoter of rat heat shock 70 kDa protein 1B (Hspa1b), containing a single heat shock response element; IRES, internal ribosome entry site; CMV IE/ $\beta$ -actin, cytomegalovirus immediate early and chicken  $\beta$ -actin promoter; TWIGS, transient warmth-inducible genetic switch system. (b) ASML, MT450 and MTLy cells stably expressing the indicated constructs were exposed to the indicated temperatures for 10 min. Three hours later, the cells were lysed and a luciferase assay was performed. (c) ASML cells stably expressing the indicated constructs were exposed to TW at 43.5°C in a 96-well plate in a water bath for 25 min (+TW). Control cells (-TW) were left untreated. Subsequently, luciferin was added to the plate and the luciferase activity was measured every 15 min for 24 hr. (d) ASML, MT450 and MTLy cells stably expressing HSPmin-Luc were cultured for 24 hr at 37°C under normoxia or hypoxia (0.1% O<sub>2</sub>) or were exposed to 43.5°C under normoxia for 10 min (TW) followed by cultivation under normoxia and 37°C for additional 3.5 hr. Subsequently, the cells were lysed and a luciferase assay was performed. (e) ASML cells stably expressing the TWIGS constructs were cultured at 37°C under normoxia or hypoxia (0.1% O<sub>2</sub>) for 48 hr. To induce TW, the cells were exposed to 43.5°C under normoxia for 10 min, followed by cultivation under 37°C and normoxia for 48 hr. At the end of the experiment, the cells were imaged by fluorescence microscopy. Scale bar, 50  $\mu$ m. [Color figure can be viewed at [wileyonlinelibrary.com](http://wileyonlinelibrary.com)]

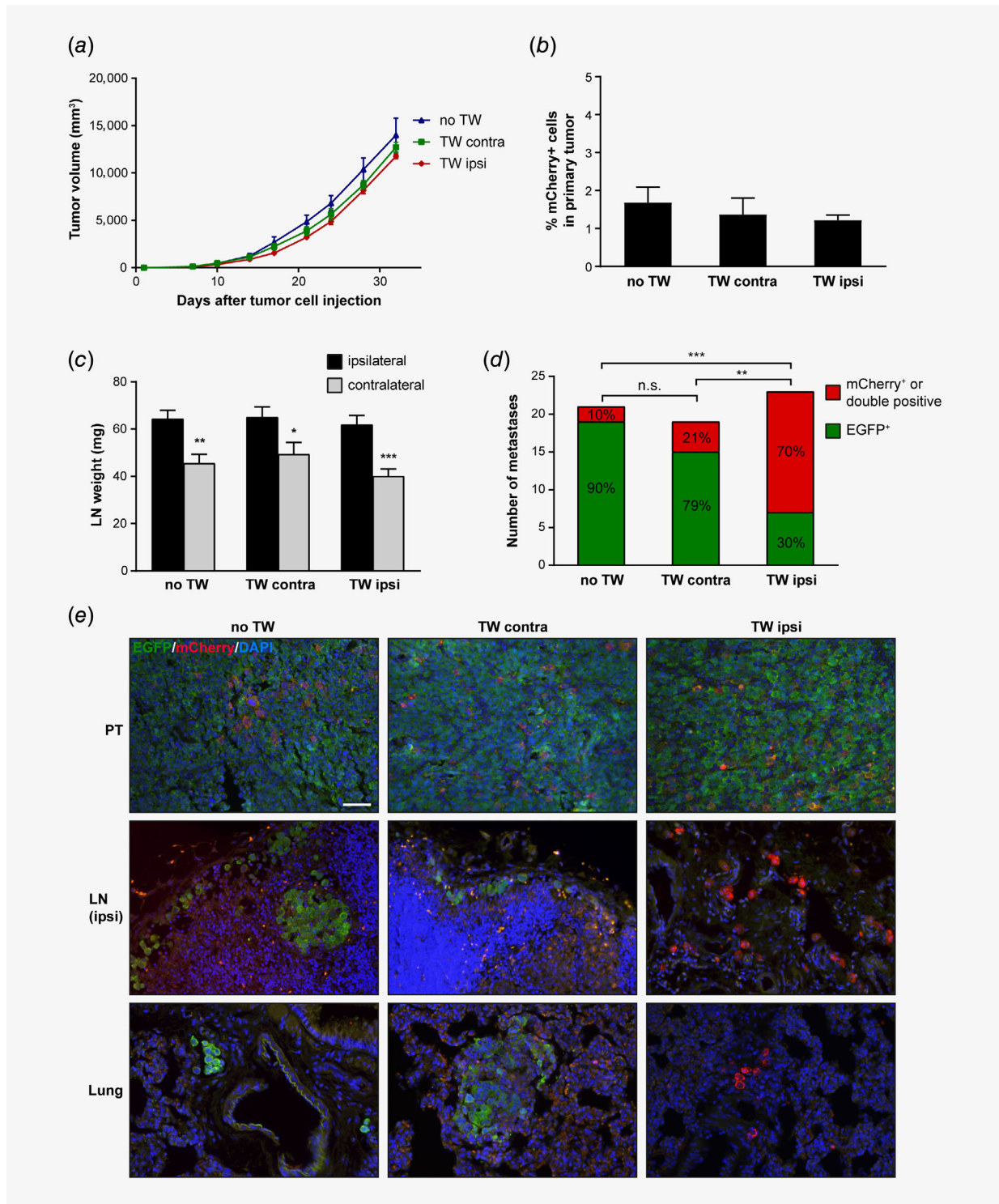


**Figure 3.** Evaluation of the contribution of tumor cells that traffic through LNs to lung metastasis. Rats were subcutaneously transplanted with ASML cells stably expressing the TWIGS constructs. Animals were either left untreated (no TW), or the lymph nodes in the contralateral (TW contra) or ipsilateral axilla (TW ipsi) were subjected to TW for 10 min daily until the end of the experiment 32 days later. (a and b) Primary tumor volume (a) and percentage of mCherry positive cells in the primary tumor (b) in the three groups ( $n = 8$ ). (c) Weight of ipsilateral and contralateral LNs in the three groups ( $n = 8$ ). (d) Number of metastases that contain EGFP-positive cells only (EGFP<sup>+</sup>) and metastases that contain mCherry-positive cells (mCherry<sup>+</sup>) in the three groups.  $**p < 0.01$ ;  $***p < 0.001$ , n.s., not significant, based on Chi-square tests between the indicated groups. (e) Immunofluorescence staining for EGFP and mCherry in primary tumors (PT), ipsilateral LNs and lungs of rats from the three groups. Scale bar, 100  $\mu\text{m}$ . [Color figure can be viewed at [wileyonlinelibrary.com](http://wileyonlinelibrary.com)]



nodes (Fig. 3c), as well as the number of surface lung metastases (Fig. 3d) was similar between the groups, indicating that TW did not affect the incidence of metastasis. However, the number of mCherry-positive metastases in the lungs of animals treated with TW on the ipsilateral side was significantly higher than that observed in animals that were untreated with TW or which received TW on the contralateral side (Figs. 3d and 3e, Supporting Information Table S1). Animals that were untreated or treated with TW on the contralateral side showed mCherry+ cells in 10 and 21% of lung metastases, respectively (Fig. 3d). In contrast, 70% of the lung metastases in animals treated with TW on the ipsilateral contained mCherry+ cells. These data allowed us to estimate that in this model at least 49% of metastases developing in the lung were seeded by cells that had trafficked *via* the axillary LNs draining the primary tumor.

### Discussion

Here we report the establishment of a tightly spatiotemporally controlled inducible genetic switch system, which allowed us to assess the contribution of tumor cell trafficking through the lymphatic system to the seeding of distant metastases. We developed a promoter element with very low basal activity that is specifically activated in a strong and sustained manner by mild TW, but not by a range of other factors in the tumor microenvironment, allowing controlled spatiotemporal induction of gene expression *in vivo* through localized time-restricted warming of tissues. The genetic switch we developed with this element should be applicable to a variety of biological and medical questions in diverse model systems that require specific inducible marking of defined populations of cells in living organisms, for example, for lineage tracing and the tracking of migratory cells. Our TW approach can be adapted to other animal models or anatomic locations, for example, by using alternative heat sources or methods such as focused ultrasound, which allows warming deep tissues.

To date, only circumstantial evidence exists regarding the relative contribution of the blood and lymphatic conduits to metastatic dissemination. Comparative analysis of the genetic evolution of primary tumors and their metastases can be used to determine the relationship between LN metastases and metastases in other organs, and thus by inference the route of dissemination, but such analyses have resulted in partially contradictory conclusions. For example, analysis of somatic variants in hypermutable DNA regions suggests that the majority of metastases in LNs and distant organs arise independently,<sup>21</sup> whereas whole-genome sequencing suggests that significant metastasis-to-metastasis spreading occurs, including from LNs.<sup>22</sup> A recent report used a photoconvertible fluorescent protein to demonstrate that tumor cells passing through LNs can be detected in the circulation and in the lungs of experimental animals.<sup>4</sup> However, the short-lived nature of the photoconverted proteins precludes the tracing of

the cells beyond a period of a few days, and thus does not allow their survival and proliferation in distant organs to be determined, nor their ability to establish overt, clinically relevant metastases. In contrast, our approach ensures permanent genetic labeling of the target cells, enabling them to be traced over extended periods to dissect their contribution to all stages of the metastatic process.

We found that around half of lung metastases that were seeded by subcutaneous tumors were derived from cells that had trafficked through the regional LNs draining the tumor. This is likely to be an underestimate, as it can take as little as 6 hr for disseminating tumor cells to transit through LNs,<sup>23</sup> and thus TW for 10 min per day likely impacted on a substantial proportion, but not all of the tumor cells disseminating *via* the lymphatic route.

A significant fraction of lung metastases that developed after TW of the ipsilateral axillary LN draining primary tumors contained both red and green cells. This is likely due to stable integration of multiple copies of the floxed EGFP-mCherry reporter construct, some of which switched in response to TW, and some of which did not, due to the transient expression of Cre recombinase. Accordingly, metastases with both red and green cells were considered to have been derived from disseminating cells that switched in response to TW of the LNs. The larger fraction of mCherry+ metastases in animals that received TW on the contralateral side, compared to animals without TW, can most probably be explained by induction of the genetic switch in tumor cells trafficking through blood vessels in the immediate vicinity of the area exposed to TW. To account for this effect, we based our estimate of the fraction of cells trafficking through the lymphatics on the difference in mCherry+ metastases between the contralateral and ipsilateral TW groups.

Our work provides direct evidence that the lymphatic vasculature can represent a major conduit for disseminating tumor cells that ultimately seed metastases in the lungs. This observation has potential clinical implications. For example, if a significant proportion of metastases are seeded by tumor cells that traffic *via* the lymphatics rather than *via* the bloodstream, then inhibiting tumor-induced lymphangiogenesis may be effective in blocking metastasis formation in vital organs. Nevertheless, we note that suppression of lymphangiogenesis in a model of colorectal cancer metastasis inhibited LN metastasis formation, but did not impact on liver metastasis formation, suggesting that the hematogenous route predominates in this model.<sup>24</sup> Similarly, specific suppression of the outgrowth of LN metastases did not inhibit lung metastasis formation in a breast cancer model.<sup>25</sup> Thus, the relative contribution of lymphogenous and hematogenous dissemination routes may vary between different types of cancer and/or depend on the exact location of the primary tumor. Future applications of the genetic marking system we present here can address these issues.



## Acknowledgements

We thank Kurt Fellenberg for the kind gift of the pPGK-Cre-bpA plasmid, Gerhard Christofori for the MMTV-IRES-Luc and pCall2-updated plasmids, Marcus Diefenbacher for the pcDNA3.1 mCherry plasmid, Christina

Warnecke for the 6xHRE-Luc plasmid and Margarete Litfin for rat genomic DNA. This work was supported by the Deutsche Forschungsgemeinschaft under the auspices of the Schwerpunktprogramm SPP1190 (Tumor-vessel interface).

## References

- Lambert AW, Pattabiraman DR, Weinberg RA. Emerging biological principles of metastasis. *Cell* 2017;168:670–91.
- Saunders TL. Inducible transgenic mouse models. *Methods Mol Biol* 2011;693:103–15.
- Adam V, Berardozi R, Byrdin M, et al. Phototransformable fluorescent proteins: Future challenges. *Curr Opin Chem Biol* 2014;20:92–102.
- Pereira ER, Kedrin D, Seano G, et al. Lymph node metastases can invade local blood vessels, exit the node, and colonize distant organs in mice. *Science* 2018;359:1403–7.
- Gomez-Pastor R, Burchfiel ET, Thiele DJ. Regulation of heat shock transcription factors and their roles in physiology and disease. *Nat Rev Mol Cell Biol* 2018;19:4–19.
- Huang Q, Hu JK, Lohr F, et al. Heat-induced gene expression as a novel targeted cancer gene therapy strategy. *Cancer Res* 2000;60:3435–9.
- Braiden V, Ohtsuru A, Kawashita Y, et al. Eradication of breast cancer xenografts by hyperthermic suicide gene therapy under the control of the heat shock protein promoter. *Hum Gene Ther* 2000;11:2453–63.
- Walther W, Stein U. Heat-responsive gene expression for gene therapy. *Adv Drug Deliv Rev* 2009;61:641–9.
- Brown M, Assen FP, Leithner A, et al. Lymph node blood vessels provide exit routes for metastatic tumor cell dissemination in mice. *Science* 2018;359:1408–11.
- Alitalo A, Detmar M. Interaction of tumor cells and lymphatic vessels in cancer progression. *Oncogene* 2012;31:4499–508.
- Sleeman J, Schmid A, Thiele W. Tumor lymphatics. *Semin Cancer Biol* 2009;19:285–97.
- Dell' Anna T, Signorelli M, Benedetti-Panici P, et al. Systematic lymphadenectomy in ovarian cancer at second-look surgery: a randomised clinical trial. *Br J Cancer* 2012;107:785–92.
- Faries MB, Thompson JF, Cochran AJ, et al. Completion dissection or observation for sentinel-node metastasis in melanoma. *N Engl J Med* 2017;376:2211–22.
- Frost JA, Webster KE, Bryant A, et al. Lymphadenectomy for the management of endometrial cancer. *Cochrane Database Syst Rev* 2017;10:CD007585.
- Giuliano AE, Ballman KV, McCall L, et al. Effect of axillary dissection vs no axillary dissection on 10-year overall survival among women with invasive breast cancer and sentinel node metastasis: the ACOSOG Z0011 (Alliance) randomized clinical trial. *JAMA* 2017;318:918–26.
- Poortmans PM, Collette S, Kirkove C, et al. Internal mammary and medial supraclavicular irradiation in breast cancer. *N Engl J Med* 2015;373:317–27.
- Whelan TJ, Olivetto IA, Parulekar WR, et al. Regional nodal irradiation in early-stage breast cancer. *N Engl J Med* 2015;373:307–16.
- Sleeman JP, Kim U, LePendu J, et al. Inhibition of MT-450 rat mammary tumour growth by antibodies recognising subtypes of blood group antigen B. *Oncogene* 1999;18:4485–94.
- Benjamin IJ, Kroger B, Williams RS. Activation of the heat shock transcription factor by hypoxia in mammalian cells. *Proc Natl Acad Sci USA* 1990;87:6263–7.
- Mestrlil R, Chi SH, Sayen MR, et al. Isolation of a novel inducible rat heat-shock protein (HSP70) gene and its expression during ischaemia/hypoxia and heat shock. *Biochem J* 1994;298 Pt5:61–9.
- Naxerova K, Reiter JG, Brachtel E, et al. Origins of lymphatic and distant metastases in human colorectal cancer. *Science* 2017;357:55–60.
- Gundem G, Van Loo P, Kremeyer B, et al. The evolutionary history of lethal metastatic prostate cancer. *Nature* 2015;520:353–7.
- Grundmann E, Vollmer E. Early local reaction and lymph node permeation of rat carcinoma HH9-cl 14 cells. An immunohistological approach. *Pathol Res Pract* 1985;179:304–9.
- Enquist IB, Good Z, Jubb AM, et al. Lymph node-independent liver metastasis in a model of metastatic colorectal cancer. *Nat Commun* 2014;5:3530.
- Quagliata L, Klusmeier S, Cremers N, et al. Inhibition of VEGFR-3 activation in tumor-draining lymph nodes suppresses the outgrowth of lymph node metastases in the MT-450 syngeneic rat breast cancer model. *Clin Exp Metastasis* 2014;31:351–65.